Available online at www.sciencedirect.com
SCIENCE DIRECT®
Journal of Chromatography A, 1063 (2005) 99–109
JOURNAL OF CHROMATOGRAPHY A
www.elsevier.com/locate/chroma

Using computer simulation to assist in the robustness analysis of an ion-exchange chromatography step

Niklas Jakobsson[a], David Karlsson[a], Jan Peter Axelsson[b], Guido Zacchi[a], Bernt Nilsson[a,*]

[a] *Department of Chemical Engineering, Lund University, P.O. Box 124, SE-22100 Lund, Sweden*
[b] *Process Development, Pfizer Health AB, SE-64541 Strängnäs, Sweden*

Received 19 July 2004; received in revised form 11 November 2004; accepted 18 November 2004

Abstract

This paper presents a methodology to gain process knowledge and assist in the robustness analysis of an ion-exchange step in a protein purification process using a model-based approach. Factorial experimental design is common practice in industry today to obtain robustness characterization of unit operations with respect to variations in process parameters. This work aims at providing a better insight into what process variations affect quality and to further reduce the experimental work to the regions of process variation that are of most interest. This methodology also greatly increases the ability to predict process performance and promotes process understanding. The model calibration part of the methodology involves three consecutive steps to calibrate a steric mass action (SMA) ion-exchange chromatography model. Firstly, a number of gradient elution experiments are performed. Secondly, experimental breakthrough curves have to be generated for the proteins if the adsorption capacity of the medium for each component is not known. Thirdly, a multi-component loading experiment is performed to calibrate the multi-component effects that cannot be determined from the single-component experiments. The separation process studied in this work is the separation of polyclonal IgG from a mixture containing IgG, myoglobin and BSA. The calibrated model is used to simulate six process variations in a full factorial experiment. The results of the simulations provide information about the importance of the different process variations and the simulations are also used to determine the crucial points for the process parameter variations. The methodology can be used to assist in the robustness analysis normally performed in the pharmaceutical industry today as it is able to predict the impact on process performance resulting from variations in salt concentration, column load, protein concentration and flow rate.

Keywords: Robustness analysis; Downstream processing; Dynamic simulation; Simulation; Steric mass action; Factorial experiment design; Ion exchange

1. Introduction

Today, when a protein purification process is to be transformed into an approved pharmaceutical production process a great deal of experimental work is performed to study the robustness of the purification process. The use of modeling and simulation in the robustness study of a process will make it possible to reduce the number of labor-intensive experiments, and thereby shorten the development time and reduce the cost. This requires a methodology employing accurate models validated by carefully designed experiments when studying a separation step in the downstream process. The methodology employed should preferably be based on an understanding of the underlying physical mechanisms of the separation process. One advantage when using this approach is that the model can be relevant for larger variations in the process parameters compared to empirical modeling.

The US Food and Drug Administration (FDA) recently published guidelines in which the importance of process un-

* Corresponding author. Tel.: +46 46 222 8088; fax: +46 46 222 4526.
E-mail address: bernt.nilsson@chemeng.lth.se (B. Nilsson).

0021-9673/$ – see front matter © 2004 Elsevier B.V. All rights reserved.
doi:10.1016/j.chroma.2004.11.067

derstanding is emphasized when validating a process [1]. These guidelines promote the use of process analytical tools such as multivariate data acquisition and analysis, modern process analyzers and process monitoring. The FDA also states that the ability to predict process behavior shows process understanding, and a greater process understanding gives more freedom in changing process conditions within the scope of the original approved validation documentation. The cost of validation often hinders process development and implementation of new process equipment in existing production processes for pharmaceuticals. The reluctance to use new process technologies in pharmaceutical industry is undesirable from a public health perspective. Efficient pharmaceutical manufacturing is of critical importance in achieving effective health care [1]. The guidelines also suggests that experimental process development databases could be used to develop process simulation tools which can contribute to gain knowledge and the reduction of the overall process development time from laboratory to production scale.

A major cost in the production of biopharmaceuticals is the cost of downstream processing. One type of protein that has attracted much attention in the biopharmaceutical industry is antibodies [2]. The antibody or the antibody fragments can be expressed in plants [3], animals [4], bacteria [5] or, most important of all, in a mammalian cell culture [6]. The high cost incurred by antibody-producing companies is due to the downstream processing, constituting 80% of the total cost [7]. Consequently, a cheap method of designing, optimizing and studying the robustness of a purification process is required.

A number of investigations have emphasized the need for a systematic approach in the validation of purification processes. In practice, this involves an extensive experimental approach [14–17]. The aim of the present study was to evaluate how a mathematical model of an ion-exchange chromatography step can be used to assist the experimental work necessary when performing a robustness study. The aim was also to use the experimental techniques normally required in process development to calibrate the model, and to keep the demand for new experiments to a minimum.

This study focuses on ion-exchange chromatography. A mixture of myoglobin, BSA and polyclonal IgG is used as a model system to evaluate the advantages of using the proposed methodology.

2. Theory—models, simulation technique and robustness analysis

The model for ion-exchange chromatography used in this study consists of a description of the interaction between the protein and solid phase and a description of the dispersion in the column. The solid-phase interaction is modeled using the steric mass action (SMA) model with interaction kinetics [8].

2.1. Modeling the external volume

To obtain the correct shape of the salt steps provided by the experimental equipment the external volume, including that of the mixing valve, has to be considered. When the external volume is greater than the column void, as was the case for the buffers that pass through a mixing valve in the experimental equipment used in this study, a modified tank series model [9] is suitable for describing the broadening effect. In order to model the salt step in elution step 1 and elution step 2 in the validation experiment, a series of perfectly mixed tanks upstream of the column was applied. Each tank was connected to a parallel tank see Eqs. (1) and (2). The number of connected tanks and the flow rate between the tanks, as well as the ratio between the volume of the tanks in the tank series and the volume of the parallel tanks, were adjusted to fit the experimental salt step using a least-squares fitting procedure.

$$\frac{\mathrm{d}c_{\mathrm{t}(i)}}{\mathrm{d}t} = \frac{F}{V_{\mathrm{t}}}(c_{\mathrm{t}(i-1)} - c_{\mathrm{t}(i)}) + \frac{F_{\mathrm{xt}}}{V_{\mathrm{t}}}(c_{\mathrm{xt}(i)} - c_{\mathrm{t}(i)}) \quad (1)$$

$$\frac{\mathrm{d}c_{\mathrm{xt}(i)}}{\mathrm{d}t} = \frac{F_{\mathrm{xt}}}{V_{\mathrm{xt}}}(c_{\mathrm{t}(i)} - c_{\mathrm{xt}(i)}) \quad (2)$$

here, $c_{\mathrm{t}(i)}$ is the concentration in tank i in the main tank series (mol/m^3), $c_{\mathrm{xt}(i)}$ the concentration in the parallel tank i (mol/m^3) (connected to tank i in the main tank series), F the volumetric flow rate in the mobile phase (m^3/s) (i.e. inlet flow to the column), F_{xt} the volumetric flow rate between the tanks in series and the parallel tanks (m^3/s), V_{t} the volume of the tanks in series (m^3) and V_{xt} the volume of the parallel tanks (m^3).

2.2. Column model

The kinetic/dispersion model describing a column contains one part describing the dispersion and convection in the mobile phase, and another part describing the adsorption. In the model used in this work, the shape of the elution peaks and breakthrough curves are dependent on a dispersion coefficient from correlation and the adsorption rate [8]. The column model for component i is described by the following equation:

$$\frac{\partial c_i}{\partial t} = D_{\mathrm{ax}}\frac{\partial^2 c_i}{\partial x^2} - v_{\mathrm{int}}\frac{\partial c_i}{\partial x} - \frac{(1-\varepsilon_{\mathrm{c}})}{\varepsilon_{\mathrm{c}}}\frac{\partial q_i}{\partial t} \quad (3)$$

where ε_{c} is the void fraction in the packed bed (m^3 mobile phase/m^3 column), x the axial coordinate along the column (m), v_{int} the interstitial velocity (m/s), D_{ax} the apparent dispersion coefficient (m^2/s), c_i the concentration of component i in the mobile phase (mol/m^3), q_i the concentration of component i in the stationary phase (mol/m^3 ion-exchange resin) and t is the time (s).

The column equation is subject to the following boundary conditions. A Robin condition describes the column inlet:

$$\frac{\partial c_i}{\partial x} = \frac{v_{\text{int}}}{D_{\text{ax}}}(c_i - c_{\text{inlet},i}) \quad \text{at } x = 0 \tag{4}$$

where $c_{\text{inlet},i}$ is the inlet concentration (mol/m^3) and c_i the concentration just inside the column (mol/m^3), which may be slightly lower than $c_{\text{inlet},i}$ due to the dispersion at the inlet. At the outlet where x is equal to L, the length of the column (m), only convective transport is considered and can thus be described by a Neumann condition (see Eq. (5)).

$$\frac{\partial c_i}{\partial x} = 0 \quad \text{at } x = L \tag{5}$$

2.3. Adsorption—the steric mass action model

The adsorption is described by steric mass action [8,10]. The interaction between protein and the solid phase in the SMA model is described as an equilibrium reaction where electro-neutrality must be conserved (see Eq. (6)). Protein and salt compete for the available binding sites on the gel. When protein binds to the gel, the binding sites on the protein occupy a number of ligands. The bound protein also shields a number of ligands due to its size.

The interaction between a number of salt ions and a protein molecule is modeled as an equilibrium reaction between the protein in the mobile phase, c_i, and the available salt ions, $\bar{q}_s$, in the gel (see Eq. (6)):

$$c_i + v_i \bar{q}_s \underset{k^*_{\text{des}}}{\overset{k^*_{\text{ads}}}{\Leftrightarrow}} q_i + v_i c_s \tag{6}$$

where c_i is the concentration in the mobile phase, q_i the concentration in the stationary phase, $\bar{q}_s$ the concentration of available sites in the gel and v the number of interacting sites between protein and gel. $k^*_{\text{ads},i}$ and $k^*_{\text{des},i}$ are the rate constants for adsorption and desorption, respectively while s and i denote salt and protein, respectively. At equilibrium, Eq. (7) is obtained.

$$\frac{k^*_{\text{des},i}}{k^*_{\text{ads},i}} = K_{\text{eq},i} = \left(\frac{c_i}{q_i}\right)\left(\frac{\bar{q}_s}{c_s}\right)^{v_i} \tag{7}$$

The concentration of unavailable salt ions, due to steric hindrance by bound protein molecules, is given by Eq. (8).

$$\hat{q}_s = \sum_{i=1}^{N} \sigma_i q_i \tag{8}$$

here $\hat{q}_s$ is the concentration of shielded ligands in the gel and N the number of interacting components. The steric factor, σ_i, describes the number of shielded ligands per bound protein molecule.

The total concentration of salt in the gel is given by adding the number of salt ions that are available on the matrix and the salt ions that are shielded by bound protein, as in Eq. (9).

$$q_s = \bar{q}_s + \hat{q}_s \tag{9}$$

The total concentration of sites in the gel can be described by:

$$\Lambda = \bar{q}_s + \sum_{i=1}^{N} (v_i + \sigma_i) q_i \tag{10}$$

and the adsorption/desorption reaction, r, can be described by Eq. (11).

$$r_i = k^*_{\text{ads},i} c_i \bar{q}_s^{v_i} - k^*_{\text{des},i} q_i c_s^{v_i} \tag{11}$$

The ratio between $k^*_{\text{ads},i}$ and $k^*_{\text{des},i}$ is determined by the equilibrium association constant, $K_{\text{eq},i}$. The result is that the interaction is modeled as a reaction at equilibrium with adsorption kinetics.

The change in protein concentration in the stationary phase is equal to the rate of the adsorption reaction.

$$\frac{\mathrm{d}q_i}{\mathrm{d}t} = r_i \tag{12}$$

The change in concentration of ligands in the gel is determined by the conservation of electro neutrality.

$$\frac{\mathrm{d}q_s}{\mathrm{d}t} = -\sum_{i=1}^{N} v_i \frac{\mathrm{d}q_i}{\mathrm{d}t} \tag{13}$$

The number of available ligands is given by combining Eqs. (8) and (9).

$$\bar{q}_s = q_s - \sum_{i=1}^{N} \sigma_i q_i \tag{14}$$

The model includes competition for the available binding sites. The protein mixture studied contains proteins of various sizes with uniformly distributed and equally accessible fixed charges at the surface as binding sites. The differences in protein size give rise to different binding conditions in different parts of the gel. Using a model without size dependence means that the effects of variation in porosity for the different proteins are not accounted for.

2.4. Model calibration

When developing an ion-exchange separation process for protein purification, the initial part of the development often consists of determining a suitable stationary phase, buffer and pH for the separation process. The methodology presented in this work comes into play when this work has been done. The first step of the methodology is to make additional gradient elution experiments at the selected pH to determine the equilibrium constant, $K_{\text{eq},i}$, and the number of interacting charges, v_i, for the SMA model [8,10,11].

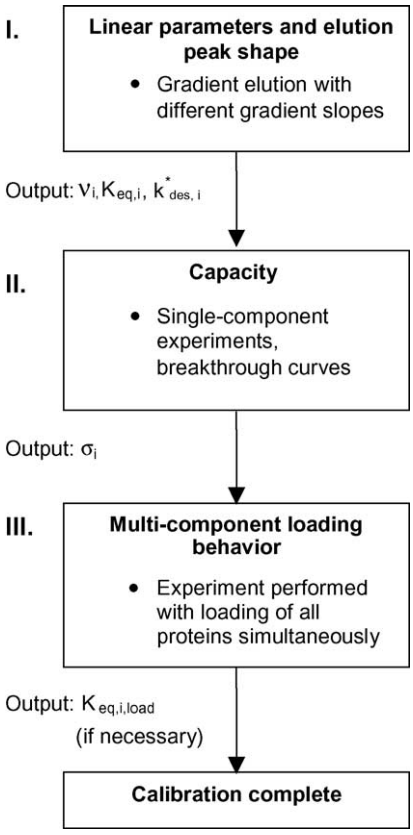

Fig. 1. Illustration of the model calibration methodology.

The shape parameter, $k^*_{des,i}$, is also adjusted to give the correct shape of the elution peaks. The second step involves single-component experiments where the capacity of each component determines the steric factor, σ, for each component [10]. The dispersion coefficient, D_{ax}, is determined by using a flow-rate-dependent correlation for column dispersion [12]. To investigate whether loading of all three proteins simultaneously gives a different result from that expected from the steric mass action model, a multi-component loading experiment is conducted. If there is a significant deviation in the position of the components breakthrough, the equilibrium constant, $K_{eq,i}$ is adjusted for each component to give an accurate simulation result. The methodology is illustrated in Fig. 1.

2.5. Simulation technique

The SMA model was implemented using a modeling and simulation tool called gPROMS developed by Process System Enterprise (London, United Kingdom) [13]. The column model was simulated using a finite-difference approximation and a fourth-order approximation for the linear solver of the resulting set of differential equations. The number of grid points in the column was set to 400 to ensure that there was no numerical broadening in the column.

2.6. Robustness analysis

A number of investigations have emphasized the need for a systematic approach in the validation of purification processes and this often implies a multivariate analysis through a factorial experimental design [14–17].

The experimental work is often conducted in laboratory scale with an appropriate scale-down from the production process. Before robustness analysis is performed, it is necessary to determine the process parameters that must be included in the study, although it may be concluded from the study that some of the parameters are unimportant for the process performance.

The normal procedure for a sensitivity analysis of product quality with respect to process variations involves several steps [14,17]. The first step is to find the normal variation in the performance of the process equipment and to determine the normal operating range (NOR) as the deviation from the normal operating point for each process parameter. The normal operating range may involve variations in flow rate, pH, conductivity, column load, etc. When the NOR has been defined from knowledge about the process equipment, laboratory experiments are usually conducted to find over what parameter range the product is able to meet the demands on purity, activity, yield, etc. This range is evaluated for variations and co-variations between the process parameters to determine the proven acceptable range (PAR) for each process parameter, which defines the limits for each process parameter that are acceptable in the process. When a process parameter variation leads to process failure, i.e. the requirement on purity or activity is not met for the parameter set, then it is said that the parameters has reached the edge of failure (EOF). Normally, only PAR and not EOF is determined in the experimental robustness analysis. The margin between NOR and PAR gives a measure of the degree of robustness of that process parameter and can be used for the classification of process parameters as critical or not, see [17].

Process parameters that are easy to control, i.e. have a narrow NOR, and process parameters that have a large influence on quality are studied for a narrower PAR. In some cases, for instance when a positive variation in a process parameter is more critical for the product quality than a negative variation, an asymmetrical range is chosen.

This work is normally conducted using factorial design experiments. When the number of process parameters is large the number of experiments has to be reduced. This can be achieved by performing a number of randomly selected experiments and from the analysis of the results the important factors can be determined and investigated further [18]. Two or three factors can also be combined into one in order to decrease the number of experiments. When there are several process parameters it is often assumed that the performance is driven primarily by some of the main effects and low-order interactions [18]. Several programs such as MODDE 7 from Umetrics (Umeå, Sweden) [19], are available to facilitate these studies.

The purpose of the present study was to develop a methodology to predict the effect of variation in process parameters on product quality, based on the understanding developed already during process development.

3. Materials and methods

3.1. Materials

The column used in the ion-exchange chromatography experiments was a strong anionexchanger, Resource 15 Q, 1 ml (no. 920408) pre-packed column (diameter 6.4 mm, length 30 mm, supplied by Amersham Biosciences (Uppsala, Sweden). The beads had a diameter of 15 μm. The column used in the gel filtration experiments was an SKW-23030 from Toso-Haas (Tokyo, Japan).

Three proteins were used in the experiments: bovine serum albumin (BSA) (A-1900, Lot no. 75H9305) and myoglobin (M-1882, Lot no. 122K7057), both obtained from Sigma (Steinheim, Germany) and polyclonal IgG, kindly provided by Biovitrum AB (Stockholm, Sweden). The latter protein solution consisted of four different types of IgG and had a concentration of 15.7% (w/w). Trizma base was obtained from Sigma and NaCl was obtained from Merck (Darmstadt, Germany).

The chromatography experiments were carried out on an ÄKTA purifier 100 system from Amersham Bioscience.

3.2. Methods

3.2.1. Experiments to determine the dead volume in the chromatography system

The ÄKTA Purifier system has a relatively low dead volume for the sample when using a 2 ml loop or a superloop in the injection of the sample. Adapting the same length of tubing as with the column and measuring the mean time for the UV response without column determined the dead volume for the sample. The dead volume between the UV detector and conductivity cell was investigated in the same manner using a solution that contained both salt and acetone and the differences in mean time between the UV and conductivity response was measured.

The dead volume in the ÄKTA Purifier system was found to be 0.14 ml, and the dead volume between the UV detector and the conductivity cell was found to be 0.4 ml.

3.2.2. Gradient elution experiments to determine the linear parameters and shape of the elution peaks

A minimum of three gradients are needed to fit the linear parameters in the SMA model [8]. The inlet concentrations used were 0.20 mg/ml IgG, 0.19 mg/ml BSA and 0.12 mg/ml myoglobin in a 20 mM Tris buffer at pH 8.7. The elution buffer was 20 mM Tris–HCl at pH 8.7 containing 1 M NaCl. The flow rate for all gradient elution experiments was 1 ml/min. The conductivity during the loading step was about 0.82 mS/cm and at the end of the gradient elution about 82 mS/cm. The loading step lasted two column volumes (CV) and the column was washed with 8.5 CV of buffer. The linear gradients used for parameter estimation were 20, 25, 30, 35, 40, 50 and 60 CV. The experimental results were compensated for dead volumes in the system to isolate the behavior due to the column.

Table 1
Protein and salt concentrations during the breakthrough experiments to determine the steric factor

Protein	Protein concentration (mg/ml)	Salt concentration (mol/dm^3)
IgG	8	0.016
BSA	8	0.030
Myoglobin	2	0.011

3.2.3. Capacity experiments to determine the steric factor

The protein and salt concentrations at the inlet are given in Table 1. The flow rate was 1 ml/min and the buffer was 20 mM Tris–HCl at pH 8.7. Some NaCl was added to obtain the salt concentrations given in Table 1.

3.2.4. Multi-component loading and elution experiment

The multi-component experiment included a loading step, column wash and two consecutive step elutions. The protein concentrations in the loading step were 3 mg/ml IgG, 0.5 mg/ml BSA and 1 mg/ml myoglobin. The conductivity in the loading step was 1.0 mS/cm and the conductivity in the equilibration and washing buffer was 0.4 mS/cm. The conductivity in the first elution step was 7.1 mS/cm, while the conductivity in the second elution step was 82 mS/cm. The flow rate was 1.2 ml/min. A sample of 12.4 ml was loaded onto the ion-exchange column and the column was washed with 4.7 ml equilibration buffer. Ten millilitres of elution buffer was used in each elution step. One millilitre Fractions were collected from each step and analyzed by gel filtration in order to determine the amount of each protein leaving the column in each step.

3.2.5. Experiments to validate the simulated robustness analysis

A full factorial experiment involving six parameters was simulated and the results are given in Table 2. To assure that the results from the simulated robustness analysis were useful for process validation, one run where low purity was expected, run 3, and two runs with a high expected purity, runs 20 and 56 in Table 2 were evaluated experimentally. The content of the first elution step in each run was evaluated regarding purity and yield of IgG.

3.2.6. Gel filtration analysis

The collected fractions were analyzed by gel filtration using the SKW-23030 column from Toso-Haas. The sample volume was 0.5 ml and the buffer used was 20 mM

Table 2
The simulated responses for a full 6-factor robustness study

Run no.	Conductivity load (%)	Conductivity wash (%)	Conductivity elu1 (%)	Conductivity elu2 (%)	Column load (%)	Flow rate (%)	Yield (%)	Purity (%)
1	−24	−24	−7	−8	−22	−11	100	90
2	+24	−24	−7	−8	−22	−11	100	93
3	**−24**	**+24**	**−7**	**−8**	**−22**	**−11**	**100**	**91**
4	+24	+24	−7	−8	−22	−11	100	93
5	−24	−24	+15	−8	−22	−11	100	90
6	+24	−24	+15	−8	−22	−11	100	93
7	−24	+24	+15	−8	−22	−11	100	91
8	+24	+24	+15	−8	−22	−11	100	93
9	−24	−24	−7	+8	−22	−11	100	90
10	+24	−24	−7	+8	−22	−11	100	93
11	−24	+24	−7	+8	−22	−11	100	91
12	+24	+24	−7	+8	−22	−11	100	93
13	−24	−24	+15	+8	−22	−11	100	90
14	+24	−24	+15	+8	−22	−11	100	93
15	−24	+24	+15	+8	−22	−11	100	91
16	+24	+24	+15	+8	−22	−11	100	93
17	−24	−24	−7	−8	+22	−11	85	96
18	+24	−24	−7	−8	+22	−11	74	96
19	−24	+24	−7	−8	+22	−11	81	96
20	**+24**	**+24**	**−7**	**−8**	**+22**	**−11**	**74**	**96**
21	−24	−24	+15	−8	+22	−11	85	96
22	+24	−24	+15	−8	+22	−11	76	96
23	−24	+24	+15	−8	+22	−11	81	96
24	+24	+24	+15	−8	+22	−11	74	96
25	−24	−24	−7	+8	+22	−11	85	96
26	+24	−24	−7	+8	+22	−11	76	96
27	−24	+24	−7	+8	+22	−11	81	96
28	+24	+24	−7	+8	+22	−11	74	96
29	−24	−24	+15	+8	+22	−11	85	96
30	+24	−24	+15	+8	+22	−11	76	96
31	−24	+24	+15	+8	+22	−11	81	96
32	+24	+24	+15	+8	+22	−11	74	96
33	−24	−24	−7	−8	−22	+11	100	90
34	+24	−24	−7	−8	−22	+11	100	93
35	−24	+24	−7	−8	−22	+11	99	92
36	+24	+24	−7	−8	−22	+11	99	94
37	−24	−24	+15	−8	−22	+11	100	90
38	+24	−24	+15	−8	−22	+11	100	93
39	−24	+24	+15	−8	−22	+11	99	92
40	+24	+24	+15	−8	−22	+11	99	94
41	−24	−24	−7	+8	−22	+11	100	90
42	+24	−24	−7	+8	−22	+11	100	93
43	−24	+24	−7	+8	−22	+11	99	92
44	+24	+24	−7	+8	−22	+11	99	94
45	−24	−24	+15	+8	−22	+11	100	90
46	+24	−24	+15	+8	−22	+11	100	93
47	−24	+24	+15	+8	−22	+11	99	92
48	+24	+24	+15	+8	−22	+11	99	94
49	−24	−24	−7	−8	+22	+11	84	96
50	+24	−24	−7	−8	+22	+11	76	96
51	−24	+24	−7	−8	+22	+11	79	96
52	+24	+24	−7	−8	+22	+11	72	96
53	−24	−24	+15	−8	+22	+11	84	95
54	+24	−24	+15	−8	+22	+11	76	96
55	−24	+24	+15	−8	+22	+11	79	96
56	**+24**	**+24**	**+15**	**−8**	**+22**	**+11**	**72**	**96**
57	−24	−24	−7	+8	+22	+11	84	96
58	+24	−24	−7	+8	+22	+11	76	96
59	−24	+24	−7	+8	+22	+11	79	96
60	+24	+24	−7	+8	+22	+11	72	96
61	−24	−24	+15	+8	+22	+11	84	95
62	+24	−24	+15	+8	+22	+11	76	96
63	−24	+24	+15	+8	+22	+11	79	96
64	+24	+24	+15	+8	+22	+11	72	96

The effects on yield and purity were calculated by changing the conductivity in the loading, washing, and the two elution steps, and also by changing the column load and flow rate. The runs marked with bold lines were evaluated experimentally. The yield is calculated as mass of IgG in the first elusion step divided by the amount of IgG that was loaded onto the column. Purity is calculated as mass of IgG in the first elution step divided by the total mass of protein eluted in the first step.

Tris–HCl at pH 8.5 containing 0.5 M NaCl. The flow rate was 0.5 ml/min and the peaks were integrated and converted from absorbance units to mg/ml using a linear relationship.

4. Results and discussion

4.1. Model calibration

4.1.1. UV-response calculation

The response in breakthrough and elution is given by the model in mol/m^3, which can be converted to mg/ml using the molecular mass. Experienced scientists working with chromatography are used to observing their breakthrough curves and elution peaks in terms of UV absorption. Therefore, experiments to determine the UV absorption for each protein at different concentrations were performed and a linear relation between UV absorption in the ÄKTA purifier UV cell and protein concentration was derived for each protein. The conversion factors were 308 ml mg/mAU for IgG, 267 ml mg/mAU for BSA and 127 ml mg/mAU for myoglobin. The UV response is used in all figures comparing simulated and experimental data, assuming that the total UV response is strictly additive for the components included in the simulation.

4.1.2. Void fraction

The Resource 15 Q column contains monosized particles with very large pores, which make it difficult to measure the column void with, for example, latex particles. Therefore, the column void was not measured experimentally. The column void fraction was set to 0.32 in the model. This is a relatively low value but it was considered reasonable as the column was industrially packed.

4.1.3. Calculation of salt concentration in the parameter estimation

The buffers used in the gradient elution experiments and in the breakthrough experiments had different conductivities. The conductivity of the sample and of the loading and elution buffers was measured. A linear relationship between salt concentration and conductivity was assumed. The 20 mM Tris buffer itself has a conductivity of 0.1 mS/cm. The conductivity in the Tris–HCl is considered to be due to the interacting salt component, which is reasonable considering that the desired pH in the buffers was achieved by adding HCl.

4.1.4. Modeling the external volume

The best fit to the experimental salt steps was achieved with seven tanks each with one parallel tank. The flow to the parallel tank was determined to be 28% of the flow through the column, and the ratio between the volume of the tanks in the tank series and the volume of the parallel tanks were 0.64 for the first elution step. In the second elution step, the flow between the tank series and the parallel tanks was 22% of the flow through the column, and the ratio between the volume of the tanks in series and the volume of the parallel tanks was determined to be 0.58. Simulated and experimental salt steps are shown in Fig. 2.

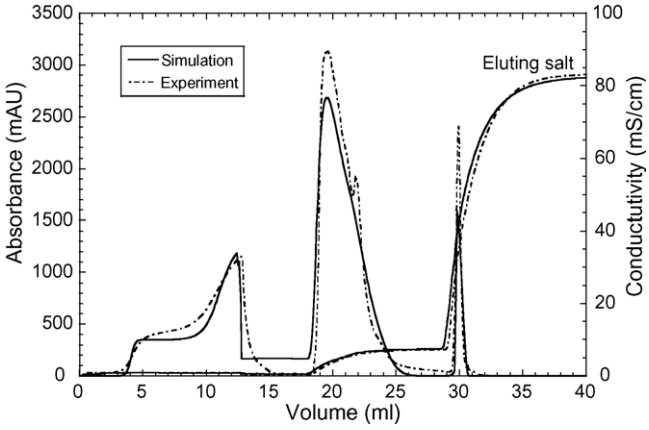

Fig. 2. Simulated and experimental chromatograms for the multi-component experiment where the equilibrium constant (K_{eq}) for myoglobin in the loading step has been adjusted in order to fit the loading part of the experiment.

4.1.5. Column dispersion

To determine the dispersion in the column an empirical correlation using the particle Peclet number was implemented to calculate the dispersion coefficient. The peclet, *Pe*, number (see Eq. (15)) was set to 0.5 [12].

$$Pe = \frac{v_{\text{int}} d_p}{D_{\text{ax}}} \tag{15}$$

here d_p is the particle diameter of the column packing. The axial dispersion coefficient in the column was found to be 4.9×10^{-8} m^2/s for a flow rate of 1 ml/min.

Breakthrough experiments were performed at a high salt content for each protein to investigate whether the broadening in the experimental runs at non-binding conditions could be used to predict the shape of the breakthrough curves and elution peaks. The breakthrough experiments were carried out at four different flow rates, 1, 2, 3, and 4 ml/min. The concentration was 0.5 mg/ml in all experiments, and a 20 mM Tris buffer with 1 M NaCl at a pH of 8.7 was used. An apparent dispersion coefficient was estimated for different flow rates for each protein. When the shape predicted by the non-binding experiments was compared to the shape of the curves and peaks at loading or gradient elution conditions it was found that the difference between using an empirical correlation and a fitted dispersion coefficient was negligible. From this, it can be concluded that the broadening effects in loading and elution are mainly due to the interactions between the protein and the solid phase, thus a dispersion coefficient determined from the correlation is sufficiently accurate.

4.1.6. Linear parameters and shape

At low protein concentration only ν_i and $K_{eq,i}$ affect the peak position in the gradient elution. The interaction rate

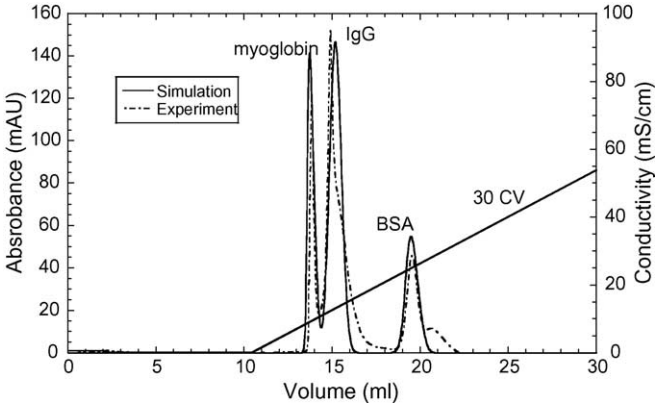

Fig. 3. Simulated and experimental chromatograms for a gradient elution of 30 column volumes.

parameter, $k^*_{\mathrm{des},i}$, is adjusted to give an accurate peak shape for the elution peaks. Fig. 3 shows that the peak shapes and positions are estimated with relatively good accuracy at 30 CV gradient elution.

The IgG used in the experiments is polyclonal and gives an asymmetrical peak. The first moment [20] of the peak was considered when estimating the peak position to give the linear parameters in the SMA model. The small peak after the BSA peak (see Fig. 3) was analyzed by gel filtration and found to be one type of IgG and this small amount of IgG was not considered in the model calibration. The various parameters that were determined for the three proteins for the SMA model are reasonable [21,22] (see Table 3). The number of interacting charges is fairly low for IgG and myoglobin. One possible explanation of this is that the pH in the buffer is fairly close to the isoelectric point of the polyclonal IgG (p*I* 6–8) and myoglobin (p*I* 7–7.5), whereas the isoelectric point for BSA is 4.8.

The mean errors on the peak position at the seven gradients (20, 25, 30, 35, 40, 50, 60 CV) used for parameter estimation were ±4.1% for IgG, ±1% for BSA and ±6.1% for myoglobin. The lower accuracy for IgG is probably due to the fact that the sample is actually polyclonal, but is considered to be one component in the model calibration. Myoglobin is more difficult to fit to this ion-exchange model than the other proteins. This could be because of the low net charge of myoglobin and the choice of pH, which lies near the isoelectric point of myoglobin. Both theses factors imply that there is a significant non-ionic mechanism involved in the solid-phase interaction for myoglobin [23], hence the large error of ±6.1%.

Table 3
The estimated values for the equilibrium constant, $K_{\mathrm{eq},i}$, the number of interacting charges, υ_i, the shape-determining interaction rate coefficient, $k^*_{\mathrm{des},i}$, and the steric factor, σ_i, are given for each protein

Protein	K_{eq} (−)	υ (−)	k^*_{des} (mol/(m^{3}s))	σ (−)
IgG	0.69	1.4	5.9×10^{-4}	446
BSA	0.17	2.2	3.4×10^{-6}	206
Myoglobin	0.77	1.1	3.1×10^{-2}	223

The total ligand density on the matrix was 265 mol/m^3 gel (obtained from the supplier).

The first moments of the gradient elution peaks were used for parameter estimation. For IgG, which contained four similar components, a perfect fit according to the first moment can give a slight difference in the position of the tip of the peak. Fig. 3 shows that the simulation fits the experimental data very well.

4.1.7. Determining the steric factor and capacity

The amount of bound protein was used to determine a steric factor. The interaction rate coefficient at loading conditions could be altered to fit the shape of the breakthrough curve. However, the multi-component loading experiment showed that the shape coefficient ($k^*_{\mathrm{des},i}$) estimated from the gradient elution experiments fitted the multi-component experiment better than the coefficient that was calculated from the single-component loading experiments. This means that only the amount of bound protein at saturation is of interest in single component experiments. Such experiments could be performed in a considerably smaller column than that normally used for process development, allowing smaller pure-component sample volumes to be used. With this method, it is not necessary to use a very high protein concentration in the loading step to algebraically calculate the steric factor from $q_{\max}$ [8,10]. The drawback of this method is the uncertainty in extrapolating the results from a lower concentration to a higher concentration. When fitting the steric factor the breakthrough curve up to 97% breakthrough was considered. The steric factor determines the equilibrium for the different proteins and should be approximately constant regardless of the concentrations of salt and protein. One drawback when extrapolating the results to the case of multi-component adsorption is that protein–protein interactions are not taken into account.

The steric factor was calculated for each protein (see Table 3). It may be considered somewhat strange that myoglobin, with a molecular weight of 17,500 g/mol, showed a higher steric factor than BSA, with molecular weight 67,000 g/mol. One explanation could be that myoglobin interacts with the matrix in a way that prevents the protein molecules from lying close to each other. Myoglobin might interact so that it covers a larger surface than implied by its molecular weight. It is also possible that this parameter value compensates for non-ion-exchange behavior that is not explained by the steric mass action model.

4.1.8. The multi-component experiment

The calibrated model was proven to accurately describe the behavior of the three proteins in the elution steps. IgG and BSA were accurately described by the single-component experiments, but myoglobin showed weaker adsorption to the column than expected. To describe the different behavior of myoglobin and get the correct breakthrough position in the loading step the equilibrium coefficient (K_{eq}) was changed

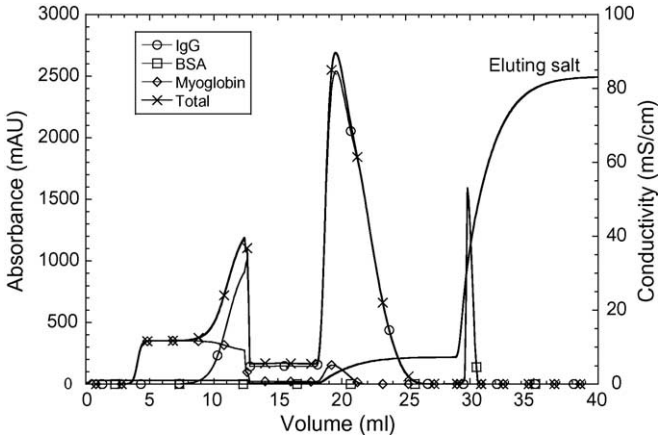

Fig. 4. The results of the simulation for each component and the simulated total UV absorbance for the multi-component loading experiment.

for from 0.77 to 2.7 for myoglobin. This resulted in a good representation of all proteins, and this adjustment was the only one needed. Fig. 2 shows a comparison between experiment and simulation.

The gel filtration analysis of the collected fractions of Fig. 2 showed that the first breakthrough contained only myoglobin, and the second increase in UV absorption of the breakthrough was due to IgG, which was beginning to leak from the column. The first part of the first elution peak contained myoglobin and the rest of the peak was IgG. The second elution peak contained only BSA. This is in accordance with the results predicted by the simulation (see Fig. 4). A small deviation in the UV response can be seen in the loading step. The model predicts a greater UV absorbance than the experiment, but in all, the model fitted the experiment very well (see Fig. 2).

4.2. Robustness analysis

The calibrated model was used to perform a full factorial study including six factors. The response to variation of the following six process parameters was studied by computer simulation.

- Conductivity in the loading step (±24%).
- Conductivity in the washing step (±24%).
- Conductivity in the first elution step (+15/−7%).
- Conductivity in the second elution step (±8%).
- Column load (±22%).
- Flow rate (±11%).

The evaluated responses were purity and yield of IgG calculated for the entire volume in the first elution step. The variations were chosen so as to represent reasonable variations in a robustness analysis in the validation of an industrial protein separation process.

In this study, rather large variations in the conductivity in the loading and washing steps were studied as the low salt concentrations at the operating point make it difficult to control the conductivity. Column load was also studied over a broad range as it can vary with the number of cycles required for each batch and with the batch size. Flow rate and conductivity in the second elution step are considered to be easier to control and were investigated over narrower ranges. An asymmetrical range was employed for the first elution step as a lower conductivity can result in a lower purity for IgG as less IgG will elute in the first step. A higher conductivity in the first elution step is less critical as BSA is far from eluting at these low conductivities.

To determine the importance of each process parameter the full factorial simulation was evaluated using MODDE 7 developed by Umetrics (Umeå, Sweden) [19]. The normal operation point was chosen to be the same as the running conditions in the multi-component experiment, but using a loading volume of 10.2 ml instead of 12.4 ml to provide a more reasonable yield at the operating point. The normal operating point gives 94.7% yield and 96% purity. The results of the robustness analysis are given in Table 2.

4.2.1. Parameter analysis

Analysis of the model response shows the importance of the different process parameters. The relative impact of each factor is shown by the height and direction of the corresponding bar in Fig. 5. Column load is an important factor for purity. This is to be expected as IgG will displace myoglobin as loading proceeds, and less myoglobin will be present in the first elution. The conductivity in the loading and washing steps has similar effects, as higher conductivity implies that less myoglobin will be adsorbed onto the column, and more myoglobin will leave the column in the loading and washing steps. As a result, less myoglobin will elute together with IgG in the first elution step. The conductivity in the first and second elution steps has low impact on product purity. Increased flow rate has a slightly positive effect on product purity as a result of a lower yield of myoglobin relative to IgG.

Fig. 5 shows that column load is the most important factor for the yield of IgG, as a higher column load leads to a greater leakage of product from the column in the loading step. Higher conductivity in the loading and washing steps also leads to a higher leakage and thus a lower yield. Flow rate also has a negative impact, as the broadening effect is increased at higher flow rates and greater broadening leads to more leakage in the loading step. The variation in the two elution steps was not high enough to cause an effect on the yield of IgG in the separation process.

4.2.2. Guidance for an experimental analysis

Table 2 shows that purity varies between 90 and 96% and the yield in the separation of IgG varies from 72 to 100%. The model-based study shows that the conductivity in the second elution step is of no importance and, can therefore be excluded from an experimental study. The analysis also showed that the conductivity in the first elution step and the flow rate are of less importance than column load, conductiv-

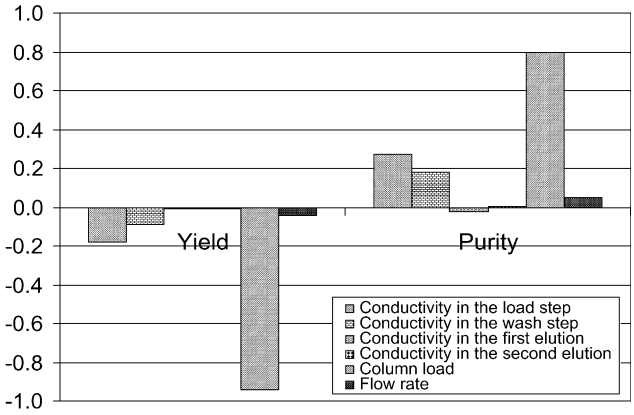

Fig. 5. The bars show the relative importance and the effect of each process parameter for product yield and purity. The numeric values on the *y*-axis are the scaled and centred coefficients in the statistical model for each variation.

ity in the loading step and conductivity in the washing step for both product purity and yield. In this the purity constraint is set to 91% and the experimental studies necessary for the validation process in this case should therefore include experiments where the purity approaches 91% or below. If purity is considered in the validation, and the conductivity in the second elution step is removed from the study, only seven parameter combinations (runs 1, 3, 5, 7, 33, 37 and 45 in Table 2) give an expected purity less than the specification, and are therefore of special interest to study experimentally. The experimental work should thus be focused on the parameter combinations that are shown to result in lower purity.

4.2.3. Validation of the simulated robustness study

The validation study was evaluated for purity and yield of IgG. Runs 3, 20 and 56 in Table 2 were evaluated experimentally and the experimental and simulated results are displayed in Table 4.

The UV absorbance was converted to mg of protein using the linear relationship described above. The results in Table 4 show that that the simulation describes the variations, as run 3 clearly results in a lower purity than run 20 and run 56, and the simulated values for product purity are in good agreement with the experimental results. The simulated yield of IgG agrees well with the experimentally determined yield for runs 20 and 56 (see Table 4). For run 3 the experimental yield is considerably smaller than expected from the simulation. The larger deviation between simulation and experiment for run 3 is probably due to myoglobin binding more strongly to the stationary phase than predicted, thereby causing a greater leakage of IgG. Although the experimental results from run 3 differ significantly from the simulation the most important aspect from a validation point of view is that the simulation can identify the runs that result in lower purity to guide the experimental study. The calibrated model accurately predicts that run 3 results in a higher yield and a lower purity than both run 20 and run 56.

Table 4
Comparison between simulated and experimental purity and yield of IgG to validate the simulated robustness analysis

Run	Purity (%) simulated	Purity (%) experimental	Yield (%) simulated	Yield (%) experimental
3	91	87	100	83
20	96	97	74	72
56	96	96	72	70

5. Conclusions

The method presented in this paper constitutes a calibrated model that succeeds in predicting the separation of three proteins: IgG, BSA and myoglobin, and can, with reasonable accuracy, predict the behavior in the ion-exchange column. It is thus reasonable to postulate that the model can provide insight into the sensitivity of process performance to variations in process parameters and in this way assist in the experimental robustness analysis of an ion-exchange column. The model can be used to investigate variations in salt concentrations, flow rate and column load. This is advantageous when studying the robustness of a separation process, as the effects of numerous combinations of process parameters can be investigated in advance by computer simulation. The experimental work can then be concentrated on the variations that are predicted to be crucial to the performance of the separation process.

It is common practice in industry to use factorial experimental design when studying process robustness. This model-based approach can provide information on how to reduce the number of factorial experiments.

To investigate the effects of a full factorial robustness analysis with six factors, a minimum of three gradient elution experiments and one breakthrough experiment for each component, together with a multi-component experiment are necessary to calibrate the ion-exchange chromatography model. Analysis of the model showed that seven process parameter

combinations gave performance less than the purity specification. The calibrated model suggests seven factorial experiments that should be evaluated experimentally in the robustness study. In conclusion, 14 experiments are needed in the methodology described in the present study where the model calibration experiments can be performed during process development, which should be compared to the 64 (+5 center points) experiments normally needed in a full factorial experiment or 32 (+5 center points) for a reduced factorial experiment.

Nomenclature

c_i	concentration of component i in the mobile phase [mol/m^3]
$c_{\text{inlet},i}$	inlet concentration of component i in the mobile phase [mol/m^3]
c_s	concentration of salt in the mobile phase [mol/m^3]
$c_{t(i)}$	concentration of salt in tank i in the tank series describing the external volume [mol/m^3]
$c_{xt(i)}$	concentration of salt in the parallel tanks connected to the tank series describing the external volume [mol/m^3]
D_{ax}	apparent dispersion coefficient [m^2/s]
d_p	bead diameter [m]
F	volume flow rate through the tank series and column [m^3/s]
F_{xt}	volume flow rate between the tank series and the parallel tanks [m^3/s]
$k^*_{\text{ads},i}$	adsorption coefficient, SMA [mol/(m^{3}s)]
$k^*_{\text{des},i}$	desorption coefficient, SMA [mol/(m^{3}s)]
$K_{\text{eq},i}$	equilibrium constant, SMA [−]
L	length of the column [m]
q_i	concentration in the stationary phase of component i [mol/m^3 gel]
q_s	total concentration of salt ligands in the gel [mol/m^3]
$\bar{q}_s$	concentration of available salt ligands in stationary phase [mol/m^3]
$\hat{q}_s$	concentration of shielded ligands [mol/m^3]
r_i	reaction rate for protein i [mol/(m^{3}s)]
t	time [s]
v_{int}	interstitial velocity [m/s]
V_t	volume of tanks used in the tank series model describing the external volume [m^3]
V_{xt}	volume of the parallel tanks connected to the tank series describing the external volume [m^3]
x	axial coordinate along the column [m]
ε_c	void fraction in the column [m^3 mobile phase/m^3 column]
η	dynamic viscosity [Pa s]
Λ	total concentration of binding sites in the gel [mol/m^3 gel]
υ_i	number of interacting sites between component i and gel [−]
σ_i	steric factor of component i [−]

Acknowledgements

The Swedish Center for BioSeparation is gratefully acknowledged for financial support. BioInvent International AB, Lund, Sweden and Biovitrum AB, Stockholm, Sweden are also acknowledged for providing materials.

References

[1] FDA, US Department of Health and Human Services, Guidance for Industry PAT: A Framework for Innovative Pharmaceutical Manufacturing and Quality Assurance, 2004.
[2] G. Walsh, Eur. J. Pharm. Biopharm. 55 (2003) 3.
[3] E. Stoger, M. Sack, R. Fischer, P. Christou, Curr. Opin. Biotechnol. 13 (2002) 161.
[4] D.P. Pollock, J.P. Kutzko, E. Birck-Wilson, J.L. Williams, Y. Echelard, H.M. Meade, J. Immunol. Methods 231 (1999) 147.
[5] H.E. Chadd, S.M. Chamow, Curr. Opin. Biotechnol. 12 (2001) 188.
[6] H. Graf, J.-N. Rabaud, J.-M. Egly, J. Immunol. Methods 139 (1991) 135.
[7] B. Hunt, C. Goddard, A.P.J. Middelberg, B.K. O'Neill, Biochem. Eng. J. (2001) 135.
[8] D. Karlsson, N. Jakobsson, K.-J. Brink, A. Axelsson, B. Nilsson, J. Chromatogr. A 1033 (2004) 71.
[9] P. Persson, H. Kempe, G. Zacchi, B. Nilsson, Chem. Eng. Res. Des. 82 (A2) (2004) 1.
[10] C.A. Brooks, S.M. Cramer, AIChE J. 38 (1992) 1969.
[11] S.D. Gadam, G. Jayaraman, S.M. Cramer, J. Chromatogr. 630 (1993) 37.
[12] T.K. Sherwood, R.L. Pigford, C.R. Wilke, Mass Transfer, McGraw-Hill, 1975.
[13] Process Systems Enterprise Ltd., gPROMS Advanced User Guide, Process Systems Enterprise Ltd., Bridge Studios, 107a Hammersmith Bridge Road, London W69DA, UK, 2001.
[14] B. Kelly, D. Jennings, P. Wright, R. Briasco, Biopharmaceutics (1997) 36.
[15] C.A. Knaack, A.M.J. Hawrylechko, Pharm. Sci. Technol. Today 7 (1998) 300.
[16] B. Wolk, P. Bezy, R. Arnold, G. Blank, Bioprocess Int. (2003) 50.
[17] R.J. Seely, H.V. Hutchins, M.P. Luscher, K.S. Sniff, R. Hassler, Biopharmaceutics (1999) 33.
[18] D.C. Montgomery, Design and Analysis of Experiments, 1997.
[19] Umetrics AB, Users Guide to Modde, 2003.
[20] O. Levenspiel, The Chemical Reactor Omnibook, OSU Book Stores, Corvallis, Oregon 97339, 1996 (Chapters 61–68, 61.1).
[21] V. Natarajan, W. Bequette, S.M. Cramer, J. Chromatogr. A 876 (2000) 51.
[22] H. Iyer, S. Tapper, P. Lester, B. Wolk, R. van Reis, J. Chromatogr. A 832 (1999) 1.
[23] M. Frost Ebershold, A.L. Zydney, Biotechnol. Progr. 85 (2004) 166.